Published in final edited form as:
J Low Temp Phys. 2016 July ; 184(1-2): 389–395. doi:10.1007/s10909-015-1373-z.

Developments in Time-Division Multiplexing of X-ray Transition-Edge Sensors

W.B. Doriese,
National Institute of Standards and Technology, Boulder, CO 80305, USA

K.M. Morgan,
National Institute of Standards and Technology, Boulder, CO 80305, USA

D.A. Bennett,
National Institute of Standards and Technology, Boulder, CO 80305, USA

E.V. Denison,
National Institute of Standards and Technology, Boulder, CO 80305, USA

C.P. Fitzgerald,
National Institute of Standards and Technology, Boulder, CO 80305, USA

J.W. Fowler,
National Institute of Standards and Technology, Boulder, CO 80305, USA

J.D. Gard,
National Institute of Standards and Technology, Boulder, CO 80305, USA

J.P. Hays-Wehle,
National Institute of Standards and Technology, Boulder, CO 80305, USA

G.C. Hilton,
National Institute of Standards and Technology, Boulder, CO 80305, USA

K.D. Irwin,
Stanford University Department of Physics, Stanford, CA 94305, USA

Y.I. Joe,
National Institute of Standards and Technology, Boulder, CO 80305, USA

J.A.B. Mates,
National Institute of Standards and Technology, Boulder, CO 80305, USA

G.C. O'Neil,
National Institute of Standards and Technology, Boulder, CO 80305, USA

C.D. Reintsema,
National Institute of Standards and Technology, Boulder, CO 80305, USA

N.O. Robbins,
National Institute of Standards and Technology, Boulder, CO 80305, USA

D.R. Schmidt,
National Institute of Standards and Technology, Boulder, CO 80305, USA

NIST Author Manuscript

NIST Author Manuscript

D.S. Swetz,
National Institute of Standards and Technology, Boulder, CO 80305, USA

H. Tatsuno,
National Institute of Standards and Technology, Boulder, CO 80305, USA

L.R. Vale, and
National Institute of Standards and Technology, Boulder, CO 80305, USA

J.N. Ullom
National Institute of Standards and Technology, Boulder, CO 80305, USA

W.B. Doriese: doriese@nist.gov

Abstract

Time-division multiplexing (TDM) is a mature scheme for the readout of arrays of transition-edge sensors (TESs). TDM is based on superconducting-quantum-interference-device (SQUID) current amplifiers. Multiple spectrometers based on gamma-ray and X-ray microcalorimeters have been operated with TDM readout, each at the scale of 200 sensors per spectrometer, as have several astronomical cameras with thousands of sub-mm or microwave bolometers. Here we present the details of two different versions of our TDM system designed to read out X-ray TESs. The first has been field-deployed in two 160-sensor (8 columns × 20 rows) spectrometers and four 240-sensor (8 columns × 30 rows) spectrometers. It has a three-SQUID-stage architecture, switches rows every 320 ns, and has total readout noise of 0.41 $\mu\Phi_0/\sqrt{\text{Hz}}$. The second, which is presently under development, has a two-SQUID-stage architecture, switches rows every 160 ns, and has total readout noise of 0.19 $\mu\Phi_0/\sqrt{\text{Hz}}$. Both quoted noise values are non-multiplexed and referred to the first-stage SQUID. In a demonstration of this new architecture, a multiplexed 1-column × 32-row array of NIST TESs achieved average energy resolution of 2.55±0.01 eV at 6 keV.

Keywords

SQUID; transition-edge sensor; time-division multiplexer; microcalorimeter; X-ray

1 Introduction

Arrays of transition-edge sensors (TESs), with spectral resolution of a few eV and collecting efficiency several orders of magnitude higher than that of conventional dispersive spectrometers, are becoming the detectors of choice in a growing variety of X-ray-spectroscopic experiments. A key supporting technology is cryogenic-multiplexed readout: because of the low operating temperatures (in systems described here, about 65 mK) and limited cooling power at these temperatures (typically, hundreds of nW via a pulse-tube-backed adiabatic-demagnetization refrigerator, or ADR), every wire from and every amplifier element in the cryogenic detector package represent important, incremental heat loads. For TES arrays larger than tens of pixels, multiplexed readout–in which multiple TES sensors share an amplifier element and its readout wiring–is essential.

Here we describe two different versions of a time-division multiplexing (TDM) architecture [1, 2] that are based on superconducting-quantum-interference-device (SQUID) current amplifiers. The first version has been field-deployed in multiple scientific spectroscopy systems, while the second is more developmental in nature. In TDM, the TESs are dc-biased, each TES is coupled to its own first-stage SQUID (SQ1), *rows* of SQ1s are switched on one at a time, and *columns* of SQUIDs are read out in parallel. The two most important metrics of performance in a SQUID-TDM readout system are (1) the row-dwell time, t_{row} (faster row switching is better) and (2) the readout noise, $s_{\varphi 1}$, which is usually expressed as the non-multiplexed noise of the entire system and referred to flux in SQ1 (lower noise is better).

2 Mature TDM Architecture

Our first TDM version for X-ray TESs is highly mature and has been fielded in six X-ray spectrometers. These deployed spectrometers include two for soft-X-ray synchrotron beamlines [3] (an 8-column × 30-row array for emission and partial-fluorescence-yield absorption spectroscopy at the National Synchrotron Light Source's beamline U7A that will soon be moved to NSLS-II beamline ID-7, and an 8 × 30 array for energy-resolved resonant scattering at the Advanced Photon Source's beamline 29-ID), two for time-resolved hard-X-ray absorption spectroscopy (an 8 × 30 array in a lab at NIST [4] and an 8 × 20 array in a lab at the Lund Kemicentrum [5]), an 8 × 20 array for particle-induced X-ray emission[6] at the Jyväskylä Pelletron accelerator, and an 8 × 30 array for spectroscopy of pionic atoms[7] at beamline π-M1 of the Paul Scherrer Institute. A paper describing these full spectroscopy systems in more detail is in preparation.

The mature TDM system is based on a three-SQUID-stage architecture (see Fig. 1). In the full system, the analog portion of each of the eight readout columns consists of a 3 mm × 20 mm microfabricated multiplexer chip (code-named "mux11c"; contains the SQ1s and the second-stage SQUID, or SQ2), an 11 mm × 19 mm microfabricated "interface" chip (contains L_{Ny} and R_{sh} for the TES-bias loops; see Fig. 1), a microfabricated SQUID array (SA)[8], and a room-temperature pre-amplifier. The mux11c and interface chips reside on the same thermal platform as the TES array (the 65 mK cold stage of a two-stage ADR), while the SA is mounted on the warmer ADR stage (about 600 mK). Total power dissipation per column is about 10 nW in the multiplexer chip, 0.5 nW in the interface chip, and 70 nW in the SA. In addition, 50 Ω termination resistors on the row-address lines dissipate a total of $\approx$ 320 nW in the warmer ADR stage.

Details of the multiplexer chip are as follows. There are 33 SQ1s per chip; in the deployed spectrometers, either 20 or 30 are used and the rest are spares. Each SQ1 is a dc SQUID with asymmetric loop inductance to give self-feedback and thus a modified sinusoidal-response curve with steeper and shallower slopes. In a recent improvement over previous versions of this three-stage architecture (e.g., [9]), we increased the dynamic resistance ($R_{dyn} = \mathrm{d}V_{SQ}/\mathrm{d}I_{SQ}$) of the SQ2 from 3 to 6 Ω by increasing the resistance of the shunts across the junctions, while reducing the junction size to reduce the parasitic capacitance. Combined with the total loop inductance (the SA-input inductance plus the inductance of the twisted-pair wiring between ADR stages) of about 225 nH, this creates a single-pole, low-pass response in the SQ2-bias loop with $f_{3dB} \approx 4$ MHz.

The SA (code-named "SA13ax") is of a "banked" design: there are six banks; each consists of 64 dc SQUIDs. The six banks are designed to be wired, via minor lithographic variations, in (series × parallel) combinations of 3 × 2, 2 × 3, and 1 × 6 to vary R_{dyn}. The deployed systems use the 2 × 3 configuration, shunted by a cryogenic R = 150 Ω chip resistor, for a combined R_{dyn} = 110 Ω. The response of the SA plus the transmission line it drives (total $C \approx$ 150 pF; unterminated at the pre-amplifier input) has a single-pole, low-pass response with $f_{\mathrm{3dB}} \approx$ 10 MHz.

The new room-temperature pre-amplifier is a simple, inexpensive circuit designed around two commercial op-amps: the Intersil EL-2125 and the Texas Instruments OPA820. The circuit has total gain of +151, input voltage noise e_{n} < 0.9 nV/√Hz, bandwidth of dc to ≈ 20 MHz, and clean response to input square waves.

The overall system has the following characteristics. The total open-loop noise is $s_{\Phi 1}$ = 0.41 $\mu\Phi_0$/√Hz (non-multiplexed; referred to SQ1). The analog open-loop bandwidth, f_{OL}, is dc to $f_{\mathrm{3dB}} \approx$ 3 MHz, which allows a row time of 320 ns: the transient due to a switch from one SQ1 to the next settles for 240 ns and then the signal is sampled for 80 ns. The fastest allowed row time of this revision of the digital-feedback electronics[10] is also 320 ns. The system is thus operated in the limit $t_{\mathrm{row}} \approx 1/f_{\mathrm{OL}}$. In this limit the multiplexed readout noise, referred to TES current, is given by[2]

$$s_{I\mathrm{TES}} = s_{\Phi 1}\sqrt{\pi N_{\mathrm{rows}}}/M_{\mathrm{in}}. \quad (1)$$

With M_{in} = 277 pH (see Fig. 1), a TES sees $s_{I\mathrm{TES}}$ = 24 pA/√Hz readout noise in the 20-row systems and 30 pA/√Hz in the 30-row systems. As an example of performance, the 8 × 30 array for pionic-atom spectroscopy [7] achieved 4.7 eV average energy resolution at 6 keV at an input count rate of 5 Hz/sensor.

3 New TDM Architecture

Our new version of TDM for X-ray TESs is designed for much higher performance, with significantly lower system noise and half the row time. Fig. 2 contains the details. The new multiplexer chip, code-named "mux13b," contains eleven SQ1 rows; the chips are designed to be chained in series to form full multiplexer columns. Each SQ1 is a four-element series array of dc SQUIDs with a flux-actuated switch. This interferometric-switch architecture was suggested by Zappe [11]. A simpler flux-actuated switch with only two junctions (and thus narrower operating margins) was previously implemented by Beyer and Drung [12]. There is no SQ2 on the multiplexer chip. Per-column power dissipation in the multiplexer chip(s) is ≈20 nW.

There are two advantages to this new architecture. The first is that the higher R_{dyn} of the multiplexer-chip output (either ≈ 40 Ω for the SQ1 biased on its steep slope or ≈ 15 Ω on its shallow slope) pushes the bandwidth of the loop connecting the chip to the SA from ≈ 4 MHz in the mature system (see Sect. 2) to at least 10 MHz. The overall system bandwidth is $f_{\mathrm{OL}} \approx$ 6 MHz, which allows the TDM rows to be switched faster: the row-to-row switching transient is reduced from 240 to 128 ns and the total row time from 320 to 160 ns. A new version of the room-temperature digital-feedback electronics is capable of switching with this faster 160 ns row-dwell time. The second advantage is that with the four-element SQ1 and without a SQ2, the multiplexer chip produces significantly lower readout noise. The total open-loop noise is $s_{\Phi 1}$ =0.19 $\mu\Phi_0/\sqrt{\mathrm{Hz}}$ with the SQ1 on its steep slope (non-multiplexed; referred to SQ1) and $s_{\Phi 1}$ =0.33 $\mu\Phi_0/\sqrt{\mathrm{Hz}}$ with the SQ1 on its shallow slope. Quadrature contributions (SQ1 on steep slope; all referred to SQ1) of the SQ1, SA, and pre-amplifier are 0.18, 0.06, and 0.05 $\mu\Phi_0/\sqrt{\mathrm{Hz}}$, respectively. With 32 rows and on the steeper SQ1 slope, the input-referred multiplexed noise is $s_{I\mathrm{TES}}$ = 16 pA/$\sqrt{\mathrm{Hz}}$ (see Eq. 1).

An initial test of the new TDM system yielded very promising results (see Fig. 3). Running at the fastest row rate (t_{row} =160 ns) allowed by the new digital-feedback crate electronics, a 1-column × 32-row array of NIST TESs achieved ΔE_{FWHM} = 2.55±0.01 eV average energy resolution at 6 keV in the 30 active sensors. Two sensors had broken wirebonds. To date, this is the highest resolution demonstration of multiplexed readout of X-ray TESs at this multiplexing scale. We are presently designing a 960-pixel (24-column × 40-row) X-ray-TES-array package around this new TDM architecture.

4 Conclusion

Time-division-SQUID multiplexing continues to be an essential readout technology for arrays of X-ray TESs. Our deployed TDM system, which has been fielded in six X-ray spectrometers, achieves 320 ns row times and readout noise of 0.41 $\mu\Phi_0/\sqrt{\mathrm{Hz}}$. It reads out 160 pixel arrays with ≈ 3.5 eV energy resolution and 240 pixel arrays with ≈ 4.5 eV resolution at 6 keV. Our new TDM system, with 160 ns row times and noise of 0.19 $\mu\Phi_0/\sqrt{\mathrm{Hz}}$, has achieved 2.55 eV resolution at 6 keV in a 32-row demonstration. It will soon bring this performance to kilopixel-scale X-ray arrays.

Acknowledgments

The cryogenic-microcalorimeter group at NASA's Goddard Spaceflight Center aided this work with frequent and fruitful discussions regarding readout of arrays of X-ray TESs as part of the Athena satellite program. We gratefully acknowledge financial support from the NASA APRA and SAT programs as well as the NIST Innovations in Measurement Science program. Mention of specific op-amps in Section 2 does not imply endorsement of these products, either by NIST or by the authors. Contribution of an agency of the United States Government; not subject to copyright.

References

1. Chervenak JA, et al. Appl Phys Lett. 1999; 74:4043.
2. Doriese WB, et al. Nucl Instrum Meth Phys Res A. 2006; 559:808.
3. Ullom JN, et al. Synchrotron Radiat News. 2014; 27:24.
4. Joe YI, et al. Proceedings of the 4th Banff Meeting on Structural Dynamics. submitted 2015; in review.
5. Uhlig J, et al. Phys Rev Lett. 2013; 110:138302. [PubMed: 23581383]
6. Palosaari M, et al. Phys Rev Appl. submitted 2015; in review.
7. Tatsuno H, et al. J Low Temp Phys. 2016 This special issue.
8. Welty RP, et al. IEEE Trans Appl Supercond. 1993; 3:2605.
9. Doriese WB, et al. Appl Phys Lett. 2007; 90:193508.

10. Reintsema CD, et al. Rev Sci Instrum. 2003; 74:4500.
11. Zappe HH. IEEE Trans Magn. 1977; 13:41–47.
12. Beyer J, Drung D. Supercond Sci Technol. 2008; 21:105022.

NIST Author Manuscript
NIST Author Manuscript

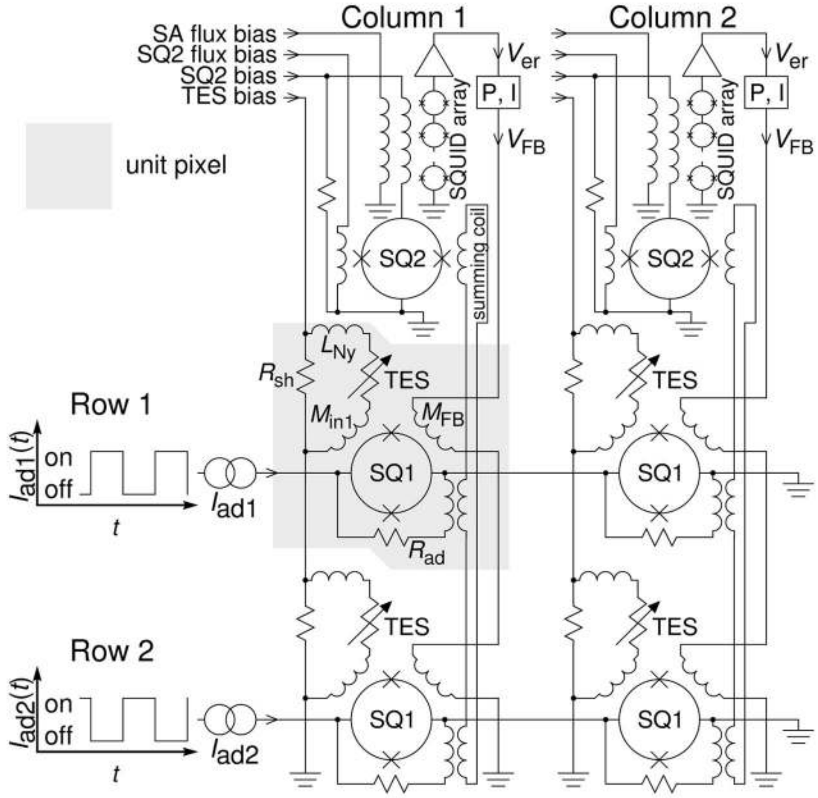

Fig. 1.

Schematic of a 2-column × 2-row TDM to represent the 8-column × 20- and 30-row TDM systems in the deployed X-ray spectrometers. Each dc-biased TES is inductively coupled (M_{in1} = 277 pH) to its own first-stage SQUID amplifier (SQ1). An inductive summing coil carries the current signals from all SQ1s in a column to a common second-stage SQUID (SQ2). Rows of SQ1s are sequentially turned on (or addressed, via I_{ad}), so the signal from one TES at a time per column is passed to that column's SQ2. Finally, the current in each SQ2 is measured by a 384-element SQUID-array amplifier, whose voltage is then amplified by a high-bandwidth, room-temperature pre-amplifier. In order to keep the nonlinear three-stage SQUID amplifier in a small, linear range, the multiplexer is run as a flux-locked loop. The pre-amplifier's output voltage, or error signal (V_{er}), is digitally sampled, and then a proportional-integral flux-feedback signal (V_{FB}) is applied inductively to the first-stage SQUIDs (M_{FB} = 32.6 pH) to servo V_{er} to a constant value. A linear combination of V_{FB} and V_{er} estimates the TES current. A crate of custom digital electronics [10] synchronizes the row-address and flux-feedback signals and streams the data to a computer.

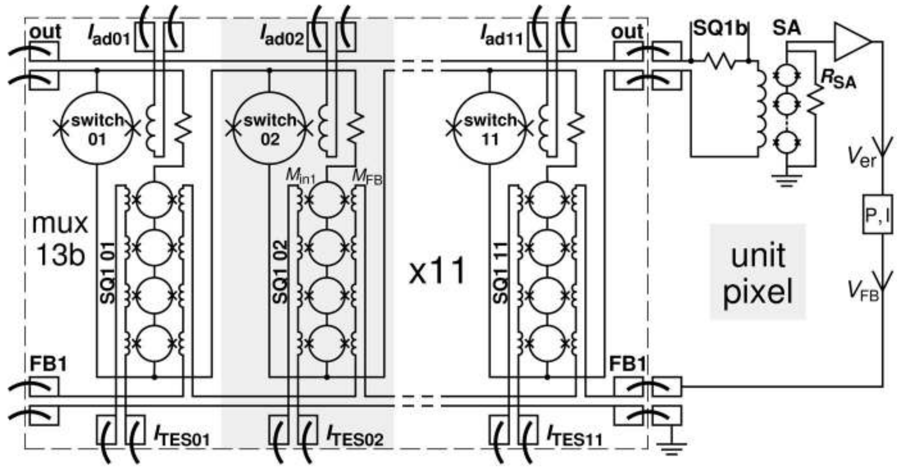

Fig. 2.
Schematic of the new TDM system. The eleven-row multiplexer chip (code-named "mux13b") contains all elements within the dashed box. Wirebonds are represented by thick arcs. Each SQ1 is a four-element series array of dc SQUIDs. Each row element is turned on (the dc voltage bias provided by "SQ1b" is routed to that row's SQ1 series array) via application of flux (current into "I_{ad}") to that row's flux-actuated-switching SQUID. With zero flux applied, the switch superconducts and shorts the SQ1b voltage. With 1/2 Φ_0 applied, the switch resistance shifts to about 100 Ω, the SQ1 element receives the SQ1b voltage, and the SQ1 achieves $R_{dyn} \approx 40\ \Omega$ (steep slope of SQ1) or $R_{dyn} \approx 15\ \Omega$ (shallow slope of SQ1). When multiple mux13b chips are chained in series (to achieve more than eleven TDM rows), the "out" and "FB1" bondpad pairs pass the bias/output and feedback signals from one chip to the next; these loops are closed via wirebond shorts of each pad pair at the end of the chain. TES signals enter via "I_{TES}." Input- and feedback-coupling values are M_{in1} = 245 pH and M_{FB} = 28.8 pH, respectively. The off-chip circuit is otherwise the same as in Fig. 1, with connection to the same shunted (R_{SA} = 150 Ω) series array (SA13ax), the same pre-amplifier, and a digital flux-locked loop.

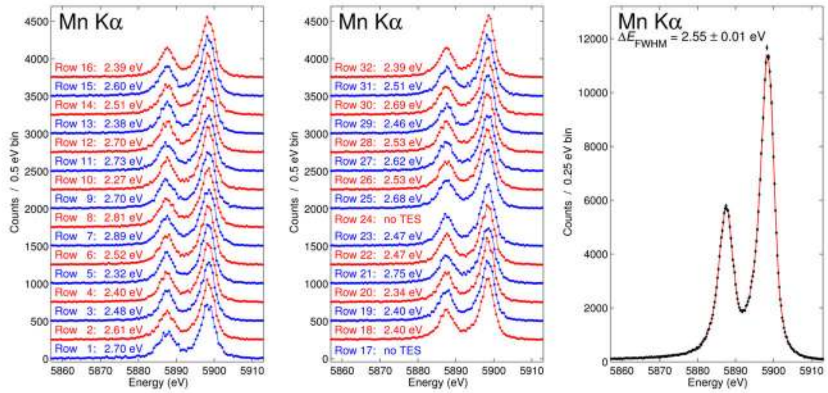

Fig. 3.

Spectra of the Mn *Kα* complex as recorded by 30 NIST X-ray TESs in a 1-column × 32-row demonstration through the new TDM system. X-rays from a broadband X-ray-tube source fluoresced a target of high-purity Mn metal chips, resulting in a flux of ≈1 Hz/sensor. Two of the TESs had broken wirebonds and thus no current signals. The TDM row time was 160 ns. The TES pulses had rising and falling exponential time constants of 60 and 1090 μs, respectively, and a maximum current slew-rate (at the pulse onset) of 0.21 A/s. The average nonmultiplexed energy resolution of the sensors was 2.4 eV at 6 keV. *Left* and *center* plots: individual spectra from TESs 1–16 and 17–32. The achieved, multiplexed energy resolution ranged from 2.27 to 2.89 eV (FWHM), with about 13,000 counts per spectrum and 1-σ statistical errors of 0.08 eV in each fit. Each histogrammed energy spectrum is offset from the last by 250 counts per 0.5 eV bin for clarity. *Right* plot: the summed energy spectrum of the 30 active TESs. Histogrammed data are in black, with one-σ vertical error bars shown. The total spectrum contains 415,000 counts. The fit to the spectral data, in red, shows energy resolution of 2.55±0.01 eV. (Color figure online.)